Available online at www.sciencedirect.com
SCIENCE DIRECT®
International Journal of Mass Spectrometry 227 (2003) 361–372
International Journal of Mass Spectrometry
www.elsevier.com/locate/ijms

New measurements of the thermochemistry of SF_5^- and SF_6^-

Kim C. Lobring, Catherine E. Check, Thomas M. Gilbert, Lee S. Sunderlin*

Department of Chemistry and Biochemistry, Northern Illinois University, DeKalb IL 60115, USA

Received 8 March 2002; accepted 27 May 2002

Abstract

Energy-resolved collision-induced dissociation (CID) experiments using a flowing afterglow-tandem mass spectrometer (MS) have been performed on SF_5^- and SF_6^-, two key components of SF_6-based plasmas. G3/B3LYP and G3(MP2) calculations have also been performed on these systems. The results are compared to other experimental and computational determinations of the thermochemistry of these species. CID of SF_5^- gives a 0 K bond energy of $D(SF_4–F^-) = 2.38 \pm 0.10$ eV (230 ± 10 kJ mol^{-1}). This is in good agreement with the high-level computational results. The threshold for dissociation of SF_6^- (into $SF_5^- + F$) of 1.85 ± 0.12 eV (178 ± 12 kJ mol^{-1}). This dissociation appears to have a barrier greater than the endothermicity, although the barrier is much smaller than that for photodetachment of the same ion.

Keywords: Thermochemistry; SF_5^-; SF_6^-; Flowing afterglow; CID

1. Introduction

Sulfur hexafluoride is used extensively as an insulating dielectric [1], in plasmas as a fluorine atom source [2] and as an etchant [3]. As an indication of the importance of SF_6, Tarnovsky et al. [1] have noted that "more than 80% of the articles [4] in the recent *Proceedings of the VIII International Symposium on Gaseous Dielectrics* deal with ... SF_6 and SF_6-containing gas mixtures." Thus, the thermodynamics of neutral and ionic species related to SF_6 are important to the modeling of plasmas. SF_6 and related molecules are also potentially significant global warming agents [5], partially because of their long atmospheric lifetimes.

Because of the relative ease of making SF_5^- and SF_6^- from SF_6, these ions have long been used as precursors in many gas-phase studies of ion chemistry [6,7]. This use is facilitated by the fact that SF_6^- is a strong fluoride donor, while SF_5^- is a relatively weak one (Table 1). Murphy and Beauchamp utilized these ions in pioneering thermochemical studies of fluoride affinities [8]. Larson and McMahon included SF_5^- in their fluoride affinity ladder, still the most comprehensive measured set of fluoride affinities [9].

Beyond its practical significance, the structure and bonding of SF_6 and related compounds are of fundamental interest. For example, attachment of an electron to SF_6 gives an SF_6^- anion with each bond stretched by 0.15 Å and vibrational frequencies lowered by an average of 45%, according to B3LYP/6-311+G(d) calculations discussed below. SF_6^- is a classic example of Franck–Condon factors; the drastic difference in

* Corresponding author. Tel.: +1-815-753-6870; fax: +1-815-753-4802.
E-mail address: sunder@niu.edu (L.S. Sunderlin).

1387-3806/03/$ – see front matter © 2003 Elsevier Science B.V. All rights reserved.
doi:10.1016/S1387-3806(03)00105-2

Table 1
Selected previous thermodynamic measurements on SF_n systems[a]

Quantity	Value		Reference
$D(SF_5–F)$	3.82 ± 0.14	Thermo	[3]
	4.35 ± 0.10	Multiple	[46]
	4.51 ± 0.10	PI	[47]
	4.62	G2	[40]
	4.64	G2(MP2)	[39]
	4.63	CCSD(T)/CBS	[37]
	3.49	BLYP/DZP^{++}	[18]
	3.69	B3LYP/DZP^{++}	[18]
	3.69	BHLYP/DZP^{++}	[18]
	3.79	BP86/DZP^{++}	[18]
	3.50	NLDF	[38]
$D(SF_4–F)$	2.51	Thermo	[3]
	1.67	G2	[40]
	1.65	G2(MP2)	[39]
	1.59	CCSD(T)/CBS	[37]
	1.53	BLYP/DZP^{++}	[18]
	1.37	B3LYP/DZP^{++}	[18]
	1.09	BHLYP/DZP^{++}	[18]
	1.72	BP86/DZP^{++}	[18]
	1.55	NLDF	[38]
$D(SF_5^-–F)$	≤1.85 ± 0.12	ERCID	This work
	1.14 ± 0.1	ERCI	[48]
	1.03	ERCID	[49]
	1.35 ± 0.1	TEA	[50]
	1.60	G3/B3LYP	This work
	1.51	G3(MP2)	This work
	1.59	G2	[36]
	1.57	G2(MP2)	[39]
	1.52	CCSD(T)/CBS	[37]
	1.97	BLYP/DZP^{++}	[18]
	1.65	B3LYP/DZP^{++}	[18]
	1.01	BHLYP/DZP^{++}	[18]
	2.11	BP86/DZP^{++}	[18]
$D(SF_4^-–F)$	4.19	G2	[36]
	4.21	G2(MP2)	[39]
	4.23	CCSD(T)/CBS	[37]
	3.77	NLDF	[38]
$D(SF_4–F^-)$	2.38 ± 0.10	ERCID	This work
	2.34 ± 0.52	IMRB	[8]
	1.90	HPMS	[9]
	2.3	HPMS(adj)	See text
	>2.60 ± 0.16	IMRB	[33]
	2.36	G3/B3LYP	This work
	2.28	G3(MP2)	This work
	2.31	G2	[36]
	2.27	CCSD(T)/CBS	[37]
	2.56	BLYP/DZP^{++}	[18]
	2.50	B3LYP/DZP^{++}	[18]
	2.41	BHLYP/DZP^{++}	[18]
	2.61	BP86/DZP^{++}	[18]
	2.90	NLDF	[38]
$EA(SF_6)$	1.07 ± 0.07	TEA	[41]
	1.05 ± 0.1	HPMS	[42]
	1.0 ± 0.2	IMRB	[43]
	1.11	G2	[36]
	1.04	G2(MP2)	[39]
	0.92	CCSD(T)/6-311G(3df)	[11]
	0.90	CCSD(T)/CBS	[37]
	3.22	BLYP/DZP^{++}	[18]
	2.66	B3LYP/DZP^{++}	[18]
	1.61	BHLYP/DZP^{++}	[18]
	3.00	BP86/DZP^{++}	[18]
$EA(SF_5)$	4.2	Thermo	[7]
	4.13	G2	[36]
	4.07	G2(MP2)	[39]
	4.08	CCSD(T)/CBS	[37]
	4.74	BLYP/DZP^{++}	[18]
	4.70	B3LYP/DZP^{++}	[18]
	4.29	BHLYP/DZP^{++}	[18]
	4.69	BP86/DZP^{++}	[18]
	4.79	NLDF	[38]
$EA(SF_4)$	1.5 ± 0.2	IMRB	[7]
	2.35 ± 0.1	IMRB	[33]
	1.63	G2	[36]
	1.52	G2(MP2)	[39]
	1.44	CCSD(T)/CBS	[37]
	2.62	BLYP/DZP^{++}	[18]
	2.45	B3LYP/DZP^{++}	[18]
	1.99	BHLYP/DZP^{++}	[18]
	2.54	BP86/DZP^{++}	[18]
	2.56	NLDF	[38]

See cited references for details of computational techniques. Experimental techniques abbreviated as follows: ERCI: energy-resolved collisional ionization; ERCID: energy-resolved collision-induced dissociation; HPMS: high pressure mass spectrometer equilibrium measurements; IMRB: ion–molecule reaction bracketing; PI: photoionization; TEA: thermal electron attachment; Thermo: thermodynamic cycle.

[a] Values in eV.

geometry means that it is not possible to photodetach an electron from SF_6^- at the adiabatic threshold near 1 eV (see Table 1). The experimental detachment energy is substantially larger, ca. 3.2 eV [10,11]. These striking effects make measurements of the thermochemistry of sulfur fluorides both a challenge and an important source of insight into the bonding of these species.

Although many experimental studies have focused on the thermochemistry of sulfur fluorides, there

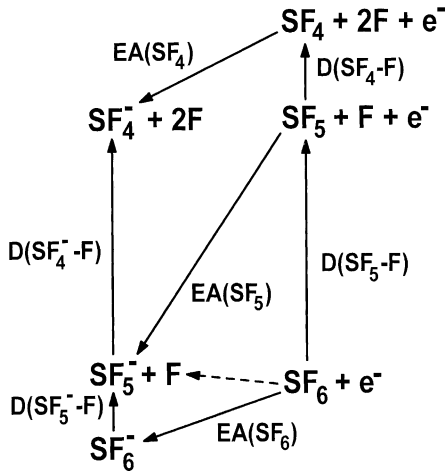

Fig. 1. Energy diagram for $SF_n^{0/-}$, $n = 4$–6. The dashed line indicates dissociative electron attachment to SF_6.

remains much uncertainty. This can be seen in Fig. 1, which shows the interconnections between bond strengths and electron affinities in the larger $SF_n^{0/-}$ species. The experimental and computed values for these quantities given in Table 1 indicate that there is still disagreement on almost every value in the system.

Energy-resolved collision-induced dissociation (CID) of SF_n^+ cations was successfully employed to derive thermochemistry by Fisher et al. [3], but analogous experiments with the anions have not been performed. This study involves measuring the energy-resolved CID of SF_6^- and SF_5^- to provide new thermochemistry. While SF_6^- is the main product of electron attachment to SF_6 at low energies, SF_5^- is the main product in the energy range between approximately 0.25 and 2.5 eV [12], making both of these ions major components in high-temperature plasmas.

Both SF_6 and SF_5^- are classic examples of hypervalent bonding [13–15], with 12 electrons around the central atom. SF_6 is octahedral; SF_5^- has the same basic structure, with a lone pair replacing a fluorine ligand. Thus, SF_5^- is of further interest as part of a program of measuring the bond strengths in hypervalent main-group halides to determine the periodic trends in these systems [16].

Hypervalent compounds are computational challenges because of the number of electrons involved and strong electron correlation effects [16,17]. Bond strengths in fluorine-containing systems in particular are difficult to calculate. High-level computational results for relevant thermochemistry are also given in Table 1. The variation in these numbers is indicative of the difficulties in calculations on these systems. For example, Schaefer and co-workers [18] derived values for the electron affinity of SF_6 ranging from 1.61 to 3.22 eV using several density functional methods. Thus, experimental measurement of the thermochemistry of SF_5^- is a useful test case for computational methods.

2. Experimental

Bond activation energies were measured using the energy-resolved CID technique [19] in a flowing afterglow-tandem mass spectrometer (MS) [20]. The instrument consists of an ion source region, a flow tube, and the tandem MS. The DC discharge ion source used in these experiments is typically set at 4000 V with 2 mA of emission current. The flow tube is a 92 cm × 7.3 cm i.d. stainless steel pipe that operates at a buffer gas pressure of 0.4 torr with a flow rate of 200 standard $cm^3\,s^{-1}$. The buffer gas is helium with up to 20% argon added to stabilize the DC discharge. The SF_6 substantially suppresses the discharge, such that a higher than usual voltage and argon flow are required to make a plasma sufficiently energetic to create a usable amount of SF_5^-.

To make the ions for this study, SF_6 was added to the ion source at a low flow rate. Electron capture produces SF_6^-, and dissociative electron capture produces a lesser amount of SF_5^-. Approximately, 10^5 collisions with the buffer gas cool the metastable ions to room temperature. SF_4^-, F^-, and a trace of SF_3^-, all higher-energy products of electron collisions with SF_6 [12], are also seen, but the amount of SF_4^- produced is insufficient for use in CID experiments.

The tandem MS includes a quadrupole mass filter, an octopole ion guide, a second quadrupole mass filter,

and a detector, contained in a stainless steel box that is partitioned into five interior chambers. Differential pumping on the five chambers ensures that further collisions of the ions with the buffer gas are unlikely after ion extraction. During CID experiments, the ions are extracted from the flow tube and focused into the first quadrupole for mass selection. The reactant ions are then focused into the octopole, which passes through a reaction cell that contains Ar collision gas. After the dissociated and unreacted ions pass through the reaction cell, the second quadrupole is used for mass analysis. The detector is an electron multiplier operating in pulse-counting mode.

The energy threshold for CID is determined by modeling the cross section for product formation as a function of the reactant ion kinetic energy in the center-of-mass (CM) frame, E_{cm}. The octopole is used as a retarding field analyzer to measure the reactant ion beam energy zero. The ion kinetic energy distribution is typically Gaussian with a full-width at half-maximum of 0.5–1.2 eV (1 eV = 96.5 kJ mol^{-1}). The octopole offset voltage measured with respect to the center of the Gaussian fit gives the laboratory kinetic energy, E_{lab}, in eV. Low offset energies are corrected for truncation of the ion beam [21]. To convert to the CM frame, the equation $E_{cm} = E_{lab}m(m + M)^{-1}$ is used, where m and M are the masses of the neutral and ionic reactants, respectively. All experiments were performed with both mass filters at low resolution to improve ion collection efficiency and reduce mass discrimination.

The total cross section for a reaction, σ_{total}, is calculated using Eq. (1), where I is the intensity of the reactant ion beam, I_o is the intensity of the incoming beam ($I_o = I + \sum I_i$), I_i is the intensity of each product ion, n is the number density of the collision gas, and l is the effective collision length, 13 ± 2 cm. Individual product cross sections σ_i are equal to σ_{total} ($I_i / \sum I_i$).

$$I = I_o \exp(-\sigma_{total} nl) \quad (1)$$

Threshold energies are derived by fitting the data to a model function given in Eq. (2), where σ(E) is the cross section for formation of the product ion at center-of-mass energy E, E_T is the desired threshold energy, σ_o is the scaling factor, n is an adjustable parameter, and i denotes rovibrational states having energy E_i and population g_i ($\sum g_i = 1$). Doppler broadening and the kinetic energy distribution of the reactant ion are also accounted for in the data analysis, which is done using the CRUNCH program written by Armentrout and co-workers [21].

$$\sigma(E) = \sigma_o \sum_i g_i \frac{(E + E_i - E_T)^n}{E} \quad (2)$$

Collisionally activated metastable complexes can have sufficiently long lifetimes that they do not dissociate on the experimental timescale (ca. 50 μs). Such kinetic shifts are accounted for in the CRUNCH program by RRKM lifetime calculations. The molecules studied in this work have moderate kinetic shifts, 0.05 and 0.17 eV, respectively for SF_5^- and SF_6^-.

Computational work on these systems was performed using the Gaussian 98 suite [22]. Several groups have previously calculated $D(SF_4–F^-)$ and $D(SF_5^-–F)$ using high-level computational techniques (Table 1). We examined these reactions using the G3(MP2) [23] and G3/B3LYP approaches [24] recently implemented into the Gaussian 98 suite. These models give absolute average deviations (AADs) from experiment within the G2 database of 0.056 and 0.043 eV, respectively, detectable improvements over the AADs of 0.082 and 0.064 eV determined for the G2(MP2) and G2 approaches.

The Atoms In Molecules (AIM) [25–27] and Natural Bond Order Analysis (NBO 5.0) [28] programs were used to calculate atomic charges. For the AIM calculations, Cartesian d functions were used for program compatibility [29].

Vibrational and rotational constants and polarizabilities for neutral molecules were calculated using the B3LYP method and the 6-311+G(d) basis set. Schaefer and co-workers have performed extensive tests of the applicability of various computational methods to anions; they found that the B3LYP method gives good results for the computational cost, although somewhat larger basis sets give better energetics [30]. The calculated and known experimental values are given in

Table 2
Calculated molecular constants[a]

Compound	Experimental vibrational (cm^{-1})[b]	Calculated vibrational (cm^{-1})[c]	Rotational (cm^{-1})[c]	Polarizability (10^{-24} cm^3)[c]
SF_6	347 (3)	314 (3)	0.0858	4.08
	525 (3)	471 (3)	0.0858	
	616 (3)	548 (3)	0.0858	6.54[d]
	642 (2)	587 (2)		
	774 (1)	684 (1)		
	948 (3)	871 (3)		
SF_6^-		95 (3)	0.0715	6.59
		210 (3)	0.0715	
		307 (3)	0.0715	
		411 (2)		
		548 (1)		
		617 (3)		
SF_5^-	241 (2)	210 (2)	0.0694	5.76
	269 (1)	222 (1)	0.1051	
	342 (1)	291 (1)	0.1051	
	435 (1)	387 (1)		
	470 (1)	394 (1)		
	[435] (2)	406 (2)		
	522 (1)	470 (1)		
	595 (2)	589 (2)		
	796 (1)	732 (1)		
SF_4	228 (1)	198 (1)	0.1004	3.94
	233 (1)	310 (1)	0.1272	
	353 (1)	413 (1)	0.2093	
	475 (1)	470 (1)		
	533 (1)	473 (1)		
	558 (1)	506 (1)		
	728 (1)	680 (1)		
	867 (1)	777 (1)		
	892 (1)	808 (1)		

[a] Numbers in parentheses are degeneracies.
[b] [2].
[c] Present work, calculated at the B3LYP/6-311+G(d) level.
[d] [31].

Table 2. The experimental polarizability for SF_6 [31] is higher than the calculated value by 60%, suggesting that the other calculated polarizabilities are also too low. However, changing the polarizabilities by 60% has a negligible effect on the derived thermochemistry ($<0.5\,kJ\,mol^{-1}$).

Because experimental determinations of the vibrational frequencies needed for the modeling are incomplete [2], the calculated values are used in the data modeling. The calculated frequencies are lower than the known experimental values [2] by $7 \pm 10\%$. However, using the experimental frequencies instead of the calculated frequencies for dissociation of SF_5^- changes the derived thermochemistry by less than 0.01 eV; the effect of changing the frequencies in the activated complex essentially cancels the effect of changing the frequencies in the transition state. Therefore, the calculated frequencies were used without scaling. Uncertainties in the derived thresholds due to possible inaccuracies in the frequencies were estimated by multiplying entire sets of frequencies for reactants, activated complexes, or transition states by

0.9 and 1.1. The resulting changes in internal energies were less than 0.04 eV. Other possible inaccuracies in transition state modeling were simulated by multiplying the time window for dissociation by 10 and 0.1. These variations change the derived thresholds by ±0.06 eV or less. These uncertainties are included in the final uncertainties of the derived thresholds. The cross sections for minor products have a negligible effect on the derived threshold values (<0.01 eV) and are not included in the fits.

An ion not sufficiently energized by one collision with the target gas may gain enough energy in a second collision to be above the dissociation threshold. This effect is eliminated by linear extrapolation of the data taken at several pressures to a zero pressure cross section before fitting the data [32].

3. Results

CID of SF_5^- and SF_6^- gives predominantly loss of fluoride anion and fluorine atom, respectively (reactions (3) and (4)). This is consistent with the order of electron affinities, EA(SF_5) > EA(F) > EA(SF_4). Two minor products, F^- and F_2^- (reactions (5) and (6)), are also seen in the dissociation of SF_6^-. Appearance curves for these reactions are shown in Figs. 2 and 3. Eq. (2) fitting parameters are given in Table 3, and the fits are shown in Figs. 2 and 3 as well. The dissociation thresholds correspond to bond activation energies at 0 K, since the effects of reactant and product internal energy are included in the fitting procedure. The final uncertainties in the energies are derived from the standard deviation of the thresholds determined for individual data sets, the uncertainty in the reactant internal energy, the effects of kinetic shifts, and the uncertainty in the energy scale (±0.15 eV lab).

Table 3
Fitting parameters for CID of SF_5^- and SF_6^- [a]

Anion	E_T (eV)	n	σ_0
SF_5^-	2.38 ± 0.09	1.27 ± 0.14	2.5 ± 0.7
SF_6^-	1.85 ± 0.10	1.09 ± 0.08	19 ± 2

[a] See text for discussion of fitting parameters.

$$SF_5^- \rightarrow SF_4 + F^- \quad (3)$$

$$SF_6^- \rightarrow SF_5^- + F \quad (4)$$

$$SF_6^- \rightarrow SF_5 + F^- \quad (5)$$

$$SF_6^- \rightarrow SF_4 + F_2^- \quad (6)$$

This gives final values of $D(SF_4–F^-) = 2.38 \pm 0.10$ eV (230 ± 10 kJ mol^{-1}) and $D(SF_5^-–F) = 1.85 \pm 0.12$ eV (179 ± 12 kJ mol^{-1}).

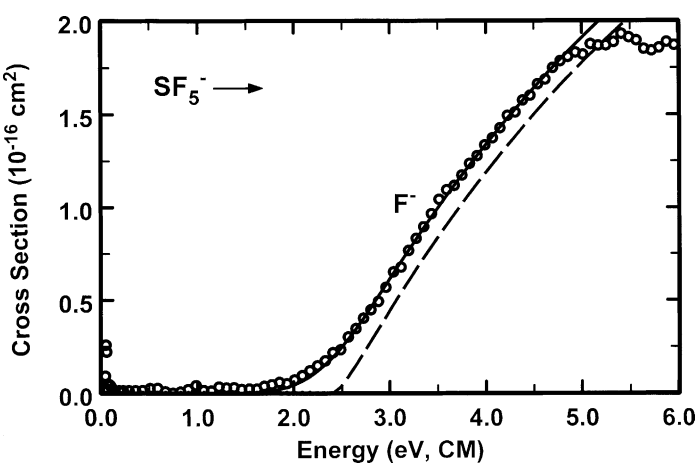

Fig. 2. Cross section for collision-induced dissociation of SF_5^- as a function of energy in the center-of-mass frame. The solid and dashed lines represent convoluted and unconvoluted fits to the data, as discussed in the text.

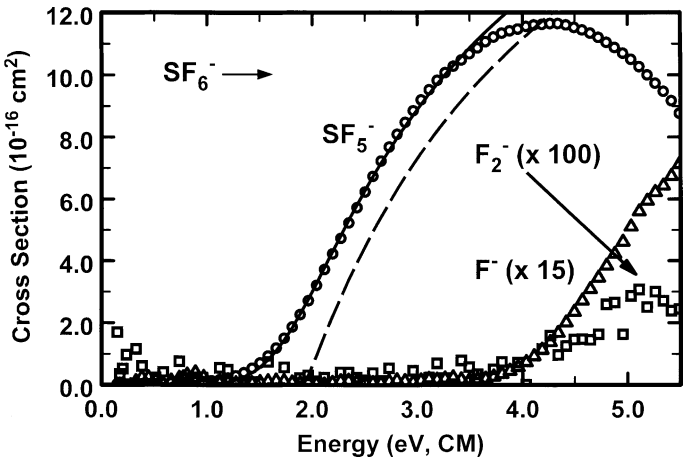

Fig. 3. Cross sections for collision-induced dissociation of SF_6^- as a function of energy in the center-of-mass frame. The solid and dashed lines represent convoluted and unconvoluted fits to the data, as discussed in the text.

In the absence of a reverse activation energy, the bond activation energy is equal to the bond strength. For the current molecules, given the substantial geometry changes discussed above, the possibility of a nonzero reverse activation energy is significant; possible barriers are discussed below.

The 0 K bond energies can be converted into 298 K bond energies and enthalpies using the heat capacities of the reactants and products. The heat capacities are determined using the frequencies calculated at the B3LYP/6-311+G(d) level (Table 2). These three thermodynamic quantities are nearly identical for both systems (Table 4). Different thermodynamic methods use different conventions; for example, electron affinities are typically 0 K values, while G(n) results are typically reported as bond energies at 298 K. Because these adjustments are significantly smaller than the experimental uncertainties, the thermochemical values in Table 1 have not been adjusted from the original reports.

Table 4
Bond dissociation thermochemistry for SF_n^- anions in kJ mol^{-1}

Bond	ΔE (0 K)	ΔE (298 K)	ΔH (298 K)
SF_4–F^-	230 ± 10	229 ± 10	232 ± 10
SF_5^-–F	≤178 ± 12	≤176 ± 12	≤178 ± 12

4. Discussion

4.1. Comparison to previous studies: $D(SF_4–F^-)$

There have been three previous experimental measurements of this bond strength. Babcock and Streit derived $D(SF_4–F^-) \geq D(SF_3–F^-) = 2.60 \pm 0.16$ eV [33]. The numerical value is marginally consistent with the present result; other values for $D(SF_3–F^-)$ give better agreement. Murphy and Beauchamp [8] reported a value of 2.34 ± 0.52 eV for the bond strength, in very good agreement considering the quoted uncertainty.

Larson and McMahon derived $D(SF_4–F^-)$=1.90 eV by using a series of equilibrium measurements of relative fluoride affinities in a high-pressure mass spectrometer (HPMS). While this method generally gives very good accuracy on relative values, absolute values on the fluoride affinity ladder depend on the accuracy of "anchors" measured through other techniques, as well as multiple individual measurements. Wenthold and Squires suggested on the basis of an absolute measurement of the fluoride affinity of HF that higher values on the fluoride affinity ladder may be consistently low by ca. 0.4 eV [34]. Adjusting the Larson and McMahon value by this amount gives a bond energy of 2.3 eV, in good agreement with the present

value of 2.38 ± 0.10 eV. New work on the fluoride affinity of SO_2, where the bond energy derived from the present technique is also ca. 0.4 eV higher than the HPMS result, discusses this issue in more detail [35].

Four groups have previously calculated $D(SF_4–F^-)$ using high-level computational techniques. The G2 value of Miller et al. [36] (2.31 eV), the CCSD(T)/CBS value of Bauschlicher and Ricca [37] (2.27 eV), and our G3(MP2) and G3/B3LYP results (2.28 and 2.36 eV) agree well with the present experimental result and with each other. The density functional values are higher than experiment by 0.03–0.23 eV; the BHLYP and B3LYP values are closer than the BLYP and BP86 values [18]. Another density functional calculation is substantially higher still [38]. The computer-intensive G(n) and CCSD(T)/CBS techniques are quite accurate; the faster density functional methods can be accurate but are not as consistent.

4.2. Thermodynamic cycles

There are three two-step paths to go from SF_5^- to $[SF_4 + F + e^-]$, as shown in reactions (7)–(9). These reactions correspond to initial loss of an electron, a fluorine atom, and a fluoride anion, respectively.

$$SF_5^- \rightarrow SF_5 + e^- \rightarrow SF_4 + F + e^- \quad (7)$$

$$SF_5^- \rightarrow SF_4^- + F \rightarrow SF_4 + F + e^- \quad (8)$$

$$SF_5^- \rightarrow SF_4 + F^- \rightarrow SF_4 + F + e^- \quad (9)$$

$$EA(SF_5) + D(SF_4–F) = D(SF_4^-–F) + EA(SF_4) = D(SF_4–F^-) + EA(F) \quad (10)$$

The sum of the energies for each of these processes is the same, giving the thermodynamic relationships in Eq. (10). Since EA(F) = 3.40 eV is well known, the present bond energy $D(SF_4–F^-) = 2.38 \pm 0.10$ eV can be added to give a value of 5.78 ± 0.10 eV for each of the sums in Eq. (10). This is in good agreement with the G2 value of 5.80 eV, the G2(MP2) value of 5.73 eV [39], and the CCSD(T)/CBS value of 5.67 eV [37]. The density functional values are quite scattered, with the BHLYP value closest to the present result (Table 1).

Table 1 indicates that most high-level calculations of $D(SF_4–F)$ give a value near 1.6 eV [37,39,40]. The previous experimental value [3] involves data from thermodynamic cycles, and some of the data included are apparently in error. Taking $D(SF_4–F) = 1.6$ eV then implies that $EA(SF_5) = 4.2$ eV. This result is in accordance with an experimental value of 4.2 eV [7] derived from thermochemical cycles. It is also in good agreement with the G2, CCSD(T)/CBS, and BHLYP calculated values given in Table 1, but the other density functional methods give values that are too high.

There are fewer data for the other sum, $D(SF_4^-–F)+EA(SF_4)$. The CCSD(T)/CBS and G2(MP2) values give values in good agreement with each other and with the experimental sum. This suggests that the individual values are accurate, and therefore that $EA(SF_4)$ is ca. 1.56 eV. This agrees well with one of the experimental values [7], but not the other [33]. Possible reasons for this discrepancy have been discussed [7]. The G2 computational value, $EA(SF_4) = 1.63$ eV [36], is also consistent, but again the density functional electron affinities are generally too high.

4.3. $D(SF_5^-–F)$

$EA(SF_6)$ has been determined experimentally to be 1.07 ± 0.07 eV [41], 1.05 ± 0.1 eV [42], and 1.0 ± 0.2 eV [43]. The average of the first two determinations has been taken to be the best available value [12], and we will use this average value of 1.06 ± 0.1 eV in this work. These results are in good agreement with the other values in Table 1 except for the density functional results; such discrepancies have been found in density functional calculations on other radical anions [30].

The dissociative electron attachment energy (DEAE) of SF_6 to form SF_5^- and F has been measured to be 0.12 ± 0.02 eV [44]. Many other studies [12] are consistent with this value, although some others give higher values such as 0.42 ± 0.02 eV [45]. The thermochemical cycle in Fig. 1 shows that the DEAE for SF_6 is equal to the difference between $EA(SF_5)$

and $D(SF_5–F)$. Taking the value $EA(SF_5) = 4.2$ eV chosen above, $D(SF_5–F) = 4.3$ or 4.6 eV, depending on which DEAE is chosen. These bracket the two direct experimental determinations, 4.35 ± 0.10 eV [46] and 4.51 ± 0.10 eV [47].

Adding $EA(SF_6)$ to $DEAE(SF_6)$ gives $D(SF_5^-–F)$= 1.2–1.5 eV. Temperature effects have not been taken into account in this result, but will not change the final bond energy significantly. The three previous experimental values listed in Table 1 [48–50] tend toward the low end of the 1.2–1.5 eV range. However, the value of $D(SF_5^-–F)$ computed using several high accuracy models, 1.5–1.6 eV (Table 1), is in agreement with the higher end of this range.

Values for $D(SF_5^-–F)$ of 1.2–1.5 eV, compared to the experimental dissociation threshold of 1.85 eV, correspond to a barrier ca. 0.3–0.6 eV higher than the reaction endothermicity. Thus, we think that the reaction threshold measured in this work corresponds to a barrier.

We attempted to model the reaction coordinate for S–F bond cleavage, locate the transition state, and determine the barrier energy by scanning the potential energy surface computationally using the B3LYP/6-31+G(d) model. This proved unsuccessful. When the dissociating fluorine atom was not constrained, it moved off the four-fold molecular axis as the S–F distance increased, and moved randomly around the quadrilateral face, which ultimately led to nonconvergence of the self-consistent field (SCF). When the fluorine was constrained to remain on the four-fold axis, the SCF converged properly at all points, but the fragments continued to show signs of wavefunction overlap even at distances greater than 10 Å; that is, the energy of the system never attained the sum of the energies of the individual fragments. Even at a distance of 24 Å, the S–F bond energy was calculated to be ca. 0.5 eV. Counterpoise calculations showed that this did not result from basis set superposition error. Furthermore, inspection of the spin density and charge matrices showed that the $[SF_5^- + F]$ and $[SF_5 + F^-]$ configurations were mixed. Thus, the dissociation of SF_6^- cannot be modeled effectively by a single configuration approach.

We are uncertain about the origin of the barrier to reaction (4), but two possible explanations follow. Both electron loss and fluorine atom loss from the 13-electron anion SF_6^- give 12-electron species (SF_6 and SF_5^-). As noted above [10,11], the threshold for photodetachment of an electron from SF_6^-, ca. 3.2 eV, is significantly in excess of $EA(SF_6) = 1.06$ eV. This barrier is attributed to substantial geometry differences between SF_6 and SF_6^-. Loss of a fluorine atom from SF_6^- gives SF_5^- where the bond length to the atom opposite the departed fluorine atom has decreased significantly [18]. This may be a cause of the presumed barrier to dissociation.

Another consideration is that the radical electron in SF_6^- is calculated to be in an orbital delocalized over the entire molecule. During dissociation, the radical electron must become localized on the departing fluorine atom. This electron interacts in an unfavorable way with the lone pair forming on the sulfur atom in SF_5^-. We note that neither of these two theories is applicable to SF_5^-, which should dissociate without a barrier [51].

4.4. AIM and NBO calculations

The inapplicability of the expanded octet model to SF_6 has been previously discussed [52], so we will compare our computational results to the three-center, four-electron (3C–4E) model [13–15]. Excluding the effects of bond polarity, the charges on the terminal atoms in 3C–4E bonds are predicted to be −0.5. The other fluorine atoms are predicted to have zero charges, and the sulfur atoms in SF_4, SF_5^-, and SF_6 are predicted to have charges of +1, +1, and +2, respectively. The additional electron in SF_6^- is delocalized over the molecule, so that expected charges on atoms in SF_6^- are not well defined. These charges can be compared to atomic charges (Table 5) derived using the AIM and NBO techniques. Previously reported AIM calculations for SF_4 and SF_6 using the MP2 model [25] also appear in this table. The results depend on the computational method chosen, but some observations are independent of method.

Table 5
Structural properties of sulfur fluoride bonds[a]

Molecule	Bond	r (Å)	q (F) (NBO)	q (F) (AIM)	q (F) (AIM)[b]	q (S) (NBO)	q (S) (AIM)	q (S) (AIM)[b]
SF_4	ax	1.705	−0.52	−0.56	−0.59	1.87	2.20	2.35
	eq	1.597	−0.41	−0.54	−0.59			
SF_5^-	ax	1.636	−0.47	−0.56		1.82	1.97	
	eq	1.792	−0.59	−0.60				
SF_6		1.607	−0.42	−0.56	−0.60	2.52	3.38	3.62
SF_6^-		1.761	−0.52	−0.53		2.13	2.20	

[a] Results calculated using B3LYP/6-311+G(d) unless otherwise noted.
[b] MP2/6-311++G** results from [25].

First, the fluoride atoms all have charges ranging from −0.4 to 0.6 using the B3LYP model. This suggests that S–F bond polarity, which is not included in the simple model, strongly affects the charge distribution. However, the differences in the charges on the axial and equatorial fluorine ligands are consistent with greater charge density on the fluorine atoms involved in 3C–4E bonding. (In SF_4, the axial fluorines are involved in 3C–4E bonding, while in SF_5^-, the four equatorial fluorines are involved in 3C–4E bonding.)

The charges on sulfur are in agreement with the prediction of the sulfur atom in SF_6 being more oxidized than in SF_4 and SF_5^-. The AIM technique gives an unusually high charge for the sulfur atom in SF_6, but not SF_6^- (indeed, the fluorine atoms in SF_6 are predicted to be more negatively charged than those in SF_6^-). It is known that AIM calculations on fluorides can be problematic [53].

5. Conclusions

The threshold for collision-induced dissociation of SF_5^- gives $D(SF_4\text{–}F^-) = 230 \pm 10\,\mathrm{kJ\,mol^{-1}}$, which we believe is the best experimental measurement of this value. The threshold for collision-induced dissociation of SF_6^-, on the other hand, appears to correspond to a barrier in excess of the endothermicity. Computional results at the G(n) and CCSD(T)/CBS levels are consistent with the available experimental results. Density functional techniques give good results in some, but not all, cases.

Acknowledgements

This work was funded by the National Science Foundation, grant CHE-9985883. We thank Peter Armentrout, Mary Rodgers, and Kent Ervin for use of the CRUNCH software for data analysis, Tom Miller and Susan Arnold for helpful advice and preliminary results, and the NIU Computational Chemistry Laboratory for computer usage.

References

[1] V. Tarnovsky, H. Deutsch, K.E. Martus, K. Becker, J. Chem. Phys. 109 (1998) 6596.
[2] C.L. Lugez, M.E. Jacox, R.A. King, H.F. Schaefer III, J. Chem. Phys. 108 (1998) 9639.
[3] E.R. Fisher, B.L. Kickel, P.B. Armentrout, J. Chem. Phys. 97 (1992) 4859.
[4] L.G. Christophorou, J.K. Olthoff (Eds.), Proceedings of the VIII International Symposium on Gaseous Dielectrics, Plenum Press, New York, 1998.
[5] W.T. Sturges, T.J. Wallington, M.D. Hurley, K.P. Shine, K. Sihra, A. Engel, D.E. Oram, S.A. Penkett, R. Mulvaney, C.A.M. Brenninkmeijer, Science 289 (2000) 611;
R.A. Kennedy, C.A. Mayhew, Int. J. Mass Spectrom. 206 (2001) i;
D.J. Jacob, Introduction to Atmospheric Chemistry, Princeton University Press, Princeton, 1999.
[6] S.T. Arnold, A.A. Viggiano, J. Phys. Chem. A 105 (2001) 3527.
[7] A.E.S. Miller, T.M. Miller, A.A. Viggiano, R.A. Morris, J.M. Van Doren, S.T. Arnold, J.F. Paulson, J. Chem. Phys. 102 (1995) 8865;
A.A. Viggiano, T.M. Miller, A.E.S. Miller, R.A. Morris, J.M. Van Doren, J.F. Paulson, Int. J. Mass Spectrom. Ion Process. 109 (1991) 327.
[8] M.K. Murphy, J.L. Beauchamp, J. Am. Chem. Soc. 99 (1977) 4992.

[9] J.W. Larson, T.B. McMahon, J. Am. Chem. Soc. 105 (1983) 2944;
J.W. Larson, T.B. McMahon, J. Am. Chem. Soc. 107 (1985) 766.
[10] R.S. Mock, E.P. Grimsrud, Chem. Phys. Lett. 184 (1991) 99;
P.G. Datskos, J.G. Carter, L.G. Christophorou, Chem. Phys. Lett. 239 (1995) 38.
[11] G.L. Gutsev, R.J. Bartlett, Mol. Phys. 94 (1998) 121.
[12] L.G. Christophorou, J.K. Olthoff, Int. J. Mass Spectrom. 205 (2000) 27.
[13] A.E. Reed, P.v.R. Schleyer, J. Am. Chem. Soc. 112 (1990) 1434.
[14] N.C. Norman, Periodicity and the P-block Elements, Oxford University Press, Oxford, 1994.
[15] E. Magnusson, J. Am. Chem. Soc. 112 (1990) 7940.
[16] K.E. Nizzi, C.A. Pommerening, L.S. Sunderlin, J. Phys. Chem. A 102 (1998) 7674;
S. Artau, K.E. Nizzi, B.T. Hill, L.S. Sunderlin, P.G. Wenthold, J. Am. Chem. Soc. 122 (2000) 10667;
B.W. Walker, C.E. Check, K.C. Lobring, C.A. Pommerening, L.S. Sunderlin, J. Am. Soc. Mass Spectrom. 13 (2002) 469.
[17] J. Moc, K. Morokuma, Inorg. Chem. 33 (1994) 551.
[18] R.A. King, J.M. Galbraith, H.F. Schaefer III, J. Phys. Chem. 100 (1996) 6061.
[19] F. Muntean, P.B. Armentrout, J. Chem. Phys. 115 (2001) 1213, and references therein.
[20] K. Do, T.P. Klein, C.A. Pommerening, L.S. Sunderlin, J. Am. Soc. Mass Spectrom. 8 (1997) 688.
[21] K.M. Ervin, P.B. Armentrout, J. Chem. Phys. 83 (1985) 166;
M.T. Rodgers, K.M. Ervin, P.B. Armentrout, J. Chem. Phys. 106 (1997) 4499.
[22] M.J. Frisch, G.W. Trucks, H.B. Schlegel, G.E. Scuseria, M.A. Robb, J.R. Cheeseman, V.G. Zakrzewski, J.A. Montgomery Jr., R.E. Stratmann, J.C. Burant, S. Dapprich, J.M. Millam, A.D. Daniels, K.N. Kudin, M.C. Strain, O. Farkas, J. Tomasi, V. Barone, M. Cossi, R. Cammi, B. Mennucci, C. Pomelli, C. Adamo, S. Clifford, J. Ochterski, G.A. Petersson, P.Y. Ayala, Q. Cui, K. Morokuma, A.D. Malick, K.D. Rabuck, K. Raghavachari, J.B. Foresman, J. Cioslowski, J.V. Ortiz, A.G. Baboul, B.B. Stefanov, G. Liu, A. Liashenko, P. Piskorz, I. Komaromi, R. Gomperts, R.L. Martin, D.J. Fox, T. Keith, M.A. Al-Laham, C.Y. Peng, A. Nanayakkara, M. Challacombe, P.M.W. Gill, B. Johnson, W. Chen, M.W. Wong, J.L. Andres, C. Gonzalez, M. Head-Gordon, E.S. Replogle, J.A. Pople, Gaussian 98, Revision A.9, Gaussian, Inc., Pittsburgh, PA, 1998.
[23] L.A. Curtiss, P.C. Redfern, K. Raghavachari, V. Rassolov, J.A. Pople, J. Chem. Phys. 110 (1999) 4703.
[24] A.G. Baboul, L.A. Curtiss, P.C. Redfern, K. Raghavachari, J. Chem. Phys. 110 (1999) 7650.
[25] J. Cioslowski, S.T. Mixon, Inorg. Chem. 32 (1993) 3209.
[26] R.F.W. Bader, Atoms in Molecules: A Quantum Theory, Clarendon Press, Oxford, 1990.
[27] J. Cioslowski, A. Nanayakkara, M. Challacombe, Chem. Phys. Lett. 203 (1993) 137;
J. Cioslowski, P.R. Surjan, J. Mol. Struc. 255 (1992) 9;
J. Cioslowski, B.B. Stefanov, Mol. Phys. 84 (1995) 707;
B.B. Stefanov, J.R. Cioslowski, J. Comp. Chem. 16 (1995) 1394;
J. Cioslowski, Int. J. Quant. Chem. Quant. Chem. Symp. 24 (1990) 15;
J. Cioslowski, S.T. Mixon, J. Am. Chem. Soc. 113 (1991) 4142;
J. Cioslowski, Chem. Phys. Lett. 194 (1992) 73;
J. Cioslowski, Chem. Phys. Lett. 219 (1994) 151.
[28] E.D. Glendening, J.K. Badenhoop, A.E. Reed, J.E. Carpenter, J.A. Bohmann, C.M. Morales, F. Weinhold, NBO 5.0, Theoretical Chemistry Institute, University of Wisconsin, Madison, WI, 2001 (http://www.chem.wisc.edu/~nbo5).
[29] http://www.chemistry.mcmaster.ca/aimpac/notes/aimweb.txt.
[30] J.C. Rienstra-Kiracofe, G.S. Tschumper, H.F. Schaefer III, S. Nandi, G.B. Ellison, Chem. Rev. 102 (2002) 231.
[31] R.D. Nelson Jr., R.H. Cole, J. Chem. Phys. 54 (1971) 4033.
[32] S.K. Loh, D.A. Hales, L. Lian, P.B. Armentrout, J. Chem. Phys. 90 (1989) 5466;
R.H. Schultz, K.C. Crellin, P.B. Armentrout, J. Am. Chem. Soc. 113 (1991) 8590.
[33] L.M. Babcock, G.E. Streit, J. Chem. Phys. 75 (1981) 3864.
[34] P.G. Wenthold, R.R. Squires, J. Phys. Chem. 99 (1995) 2002.
[35] K.C. Lobring, C.E. Check, L.S. Sunderlin, Int. J. Mass Spectrom. 222 (2003) 221.
[36] T.M. Miller, S.T. Arnold, A.A. Viggiano, Int. J. Mass Spectrom. 227 (2003) 413.
[37] C.W. Bauschlicher Jr., A. Ricca, J. Phys. Chem. A 102 (1998) 4722.
[38] G.L. Gutsev, T. Ziegler, J. Chem. Phys. 96 (1992) 7623.
[39] Y.-S. Cheung, Y.-J. Chen, C.Y. Ng, S.-W. Chiu, W.-K. Li, J. Am. Chem. Soc. 117 (1995) 9725.
[40] K.K. Irikura, J. Chem. Phys. 102 (1995) 5357.
[41] E.C.M. Chen, J.R. Wiley, C.F. Batten, W.E. Wentworth, J. Phys. Chem. 908 (1994) 88.
[42] E.P. Grimsrud, S. Chowdhury, P. Kebarle, J. Chem. Phys. 83 (1985) 1058. A slightly different value, EA(SF_6) = 1.03 eV, is found in S. Chowdhury, T. Heinis, E.P. Grimsrud, P. Kebarle, J. Phys. Chem. 90 (1986) 2747.
[43] G.E. Streit, J. Chem. Phys. 77 (1982) 826.
[44] D. Smith, P. Španěl, S. Matejcik, A. Stamatovic, T.D. Märk, T. Jaffke, E. Illenberger, Chem. Phys. Lett. 240 (1995) 481. Error limits from private communication by P. Španěl, D. Smith, in: A.E.S. Miller, T.M. Miller, A.A. Viggiano, R.A. Morris, J.M. Van Doren, S.T. Arnold, J.F. Paulson, J. Chem. Phys. 102 (1995) 8865.
[45] T.M. Miller, A.E. Stevens Miller, J.F. Paulson, J. Chem. Phys. 100 (1994) 8841.
[46] W. Tsang, J.T. Herron, J. Chem. Phys. 96 (1992) 4272.
[47] M. Evans, C.Y. Ng, C.-W. Hsu, P. Heimann, J. Chem. Phys. 106 (1997) 978.

[48] C.B. Leffert, S.Y. Tang, E.W. Rothe, T.C. Cheng, J. Chem. Phys. 61 (1974) 4929.
[49] K.M.A. Refaey, J.L. Franklin, Int. J. Mass Spectrom. Ion Phys. 26 (1978) 125.
[50] E.C.M. Chen, L.-R. Shuie, E. D'sa, C.F. Batten, W.E. Wentworth, J. Chem. Phys. 88 (1988) 4711.
[51] P.B. Armentrout, J. Simons, J. Am. Chem. Soc. 114 (1992) 8627.
[52] A.E. Reed, F. Weinhold, J. Am. Chem. Soc. 108 (1986) 3586.
[53] Æ. Frisch, M.J. Frisch, Gaussian 98, User's Reference, 2nd ed., Gaussian, Inc., 1999, p. 43.